

Transient Lymphopenia and Interstitial Pneumonia With Endotheliitis in SARS-CoV-2–Infected Macaques

Bon-Sang Koo,^{1,a} Hanseul Oh,^{1,a} Green Kim,¹ Eun-Ha Hwang,¹ Hoyin Jung,¹ Youngjeon Lee,¹ Philyong Kang,² Jae-Hak Park,³ Choong-Min Ryu,⁴ and Jung Joo Hong¹

¹National Primate Research Center, Korea Research Institute of Bioscience and Biotechnology, Cheongju, Chungcheongbuk, Republic of Korea, ²Futuristic Animal Resource Center, Korea Research Institute of Bioscience and Biotechnology, Cheongju, Chungcheongbuk, Republic of Korea, ³Department of Laboratory Animal Medicine, College of Veterinary Medicine, Seoul National University, Seoul, Republic of Korea, and ⁴Infectious Disease Research Center, Korea Research Institute of Bioscience and Biotechnology, Daejeon, Republic of Korea

Using a reliable primate model is critical for developing therapeutic advances to treat humans infected with severe acute respiratory syndrome coronavirus-2 (SARS-CoV-2). Here, we exposed macaques to high titers of SARS-CoV-2 via combined transmission routes. We observed acute interstitial pneumonia with endotheliitis in the lungs of all infected macaques. All macaques had a significant loss of total lymphocytes during infection, which were restored over time. These data show that SARS-CoV-2 causes a coronavirus disease 2019 (COVID-19)-like disease in macaques. This new model could investigate the interaction between SARS-CoV-2 and the immune system to test therapeutic strategies.

Keywords. macaques, lymphopenia, pneumonia, SARS-CoV-2.

In March 2020, the World Health Organization classified coronavirus disease 2019 (COVID-19) as a pandemic. There is an urgent need for rapid diagnosis and development of therapeutic modalities. The absence of a reliable preclinical animal model that recapitulates patients with severe acute respiratory syndrome coronavirus-2 (SARS-CoV-2) infection poses a major limitation to the development of improved diagnostics and therapeutics.

The immune system of nonhuman primates (NHPs) resembles that of humans, and the structure of the ACE2 receptor is

very similar [1]. However, current studies in NHPs infected with human coronaviruses have shown inconsistent outcomes. In SARS-CoV-2-infected macaques, previous studies reported significant lung lesions [2, 3], while others found edema and inflammation in alveoli, with mild clinical findings [4, 5]. Studies reported that SARS-CoV-2 infection resulted in no severe clinical signs, but pulmonary pneumonia was observed in 50% of cynomolgus macaques, recapitulating mild symptoms in humans [6]. However, others demonstrated that macaques showed pulmonary infiltrates and high viral loads in the lungs, suggesting moderate disease [7]. In this study, we establish a promising NHP model by addressing the following: (1) genetic and immunological variability in subspecies, (2) inoculum dose, (3) inoculum route, (4) virulent strain of virus isolated from patient, and (5) demographic background of NHPs.

METHODS

Animals and Study Design

Sixteen male and female macaques, including 8 healthy Cambodian-origin cynomolgus (*Macaca fascicularis*) and Chinese-origin rhesus macaques (*Macaca mulatta*), aged 3–6 years, were selected by the institutional veterinary experts based on their general health. All animals reared in indoor cages in the animal biosecurity level 3 (ABL-3) laboratory in the Korea National Primate Research Centre (KNPRC) at the Korea Research Institute of Bioscience and Biotechnology (KRIBB). Animals were anaesthetized with a combination of ketamine sodium (10 mg/kg) and tiletamine/zolazepam (5 mg/kg) for viral challenges, swabs, and blood collection. As illustrated in [Supplementary Figure 1A](#), all animals were challenged with a total of 12.5 mL of virus (2.1×10^6 50% tissue culture infectious doses/mL [TCID₅₀]/mL) via intratracheal (4 mL), oral (5 mL), conjunctival (0.5 mL), intranasal (1 mL), and intravenous (2 mL) route. Both cynomolgus and rhesus macaques (n = 4 each species, 2 males and 2 females) were euthanized and necropsied at 3 days post infection (dpi). After viral challenges, all live animals were subjected to swab sampling of nasopharyngeal, oropharyngeal, conjunctival, and rectal tissues, at 0, 1, and 3 dpi. All swab samples were collected in universal viral transport medium, centrifuged (1600g for 10 minutes), and filtered with 0.2- μ m pore size syringe filters for further virus quantification. Upon necropsy, tissue samples, including respiratory, immune, intestinal, cardiovascular, and reproductive organs, were grossly examined, and collected for viral detection and microscopic examination. All animal procedures were approved by the KRIBB Institutional Animal Care and Use Committee (permit number KRIBB-AEC-20064).

Received 16 June 2020; editorial decision 28 July 2020; accepted 1 August 2020; published online August 3, 2020.

^aB. S. K. and H. O. contributed equally to this work.

Correspondence: Jung Joo Hong, DVM, PhD, Korea Research Institute of Bioscience and Biotechnology, 30 Yeongudanji Street, Ochang, Cheongju-si, Chungcheongbuk-do, Republic of Korea (hong75@kribb.re.kr).

The Journal of Infectious Diseases® 2020;222:1596–600

© The Author(s) 2020. Published by Oxford University Press for the Infectious Diseases Society of America. This is an Open Access article distributed under the terms of the Creative Commons Attribution-NonCommercial-NoDerivs licence (<http://creativecommons.org/licenses/by-nc-nd/4.0/>), which permits non-commercial reproduction and distribution of the work, in any medium, provided the original work is not altered or transformed in any way, and that the work is properly cited. For commercial re-use, please contact journals.permissions@oup.com
DOI: 10.1093/infdis/jiaa486

SARS-CoV-2 Virus

A SARS-CoV-2 virus (accession number 43326) isolated from a Korean patient was obtained from the National Culture Collection for Pathogens (Cheongju, Korea). This pathogen was passaged 3 times in VERO cells. The virus titer, expressed as TCID₅₀/mL, was measured in VERO cells and determined using the Reed and Muench method. All procedures were performed in a biosafety cabinet class II in the ABL-3 facility in the KNPRC at the KRIBB (permit number KRIBB-IBC-20200206).

Virus Identification and Quantification

All tissue samples were diluted 10-fold (w/v) with sterile phosphate-buffered solution (PBS, pH 7.4) and homogenized using a Precellys Homogenizer (Bertin Instruments). After centrifugation, the supernatants were directly inoculated into VERO cells and incubated for 3 days at 37°C, for virus isolation to calculate the values of TCID₅₀/mL. The viral RNA genome was extracted from the supernatant using QIAamp Viral RNA Mini Kit (Qiagen) and stored at -80°C in the ABL-3 facility until use. Quantitative reverse transcription polymerase chain reaction (qRT-PCR) was performed with a primer set targeting partial regions of the ORF1b gene in the SARS-CoV-2 virus using the QIAGEN OneStep RT-PCR kit (Qiagen) as previously reported [8]. For all qRT-PCR analyses, SARS-CoV-2 RNA standard and negative samples were run in parallel for determination of virus copy number (see [Supplementary Material](#) for more detailed information).

Histopathology and Immunohistochemistry

For histopathological examination, all tissue samples were fixed in 10% neutral buffered formalin, embedded in paraffin, and 4- to 5- μ m sections were stained with hematoxylin and eosin. For staining of SARS-CoV-2 antigens, an immunohistochemistry assay was performed (see [Supplementary Material](#) for more detailed information).

Blood and FACS Analysis

Hematological evaluation was conducted using an autohematology analyzer (Mindray BC-5000) on examination days. Whole-blood samples were stained with antibodies. After addition of FACS lysing solution (BD Biosciences), blood cells were washed with PBS containing 2% fetal bovine serum. Peripheral blood mononuclear cells (PBMCs) and cells from tissues were washed without this lysing step. Cells were then permeabilized with BD Cytotfix/Cytoperm solution (BD Biosciences) for 20 minutes and washed with permeabilization wash buffer. Samples were incubated with anti-Ki67-fluorescein isothiocyanate (FITC), and with isotype-FITC for the control, washed, and fixed with 1% paraformaldehyde. Data were acquired with an LSRFortessa system (BD Bioscience) and analyzed using FlowJo software (v. 10 Tree Star) (see [Supplementary Material](#) for more detailed information).

Next-Generation Sequencing Analysis

Total RNA was isolated from PBMCs with TRIzol LS reagent (Invitrogen) as per the manufacturer's instructions. RNA qualification and quantitative sequence analysis of each RNA sample was performed using a customized service provided by eBiogen Inc. (Seoul, Korea) (see [Supplementary Material](#) for more detailed information).

Statistical Analysis

Group differences were determined using 1-way analysis of variance (ANOVA) with Tukey post-hoc test in Prism version 8.4.2 (GraphPad Software). Significance was set at $P < .05$.

RESULTS

To determine whether animals had depressed behavior during wake/sleep states after SARS-CoV-2 infection, the average mean locomotion activity was measured by Acticals attached to collars for 3 days before and after infection. We observed decreased activity in some animals post infection ([Supplementary Figure 1B](#)). No changes in weight or respiratory rate were observed, but most animals (13/16) showed an increase in temperature 1 dpi and returned to baseline thereafter ([Supplementary Figure 1C](#)). Post-mortem examination of all animals at 3 dpi showed multifocal, bright red lesions in the upper, middle, and lower lobes of the lungs ([Figure 1A](#)). In these pulmonary lesions, acute interstitial pneumonia (thickening of alveolar wall with type-II pneumocyte hyperplasia, mononuclear and polymorphonuclear [PMN] leukocytes infiltration) was observed ([Figure 1B](#)), similar to previous data in humans [9] and monkeys [6]. Additionally, endotheliitis was observed in the lungs of all animals (mononuclear and PMN leukocyte infiltrates within the intima of many vessels, edema of vessel, and focal hemorrhage; [Figure 1B and 1C](#)), which is in line with a recent report [10]. The viral RNA was highest in the upper respiratory swab samples and lung tissues at the earliest phase of infection, and the viral antigen was present in the lungs ([Figure 1C and 1D](#)), suggesting the predominant site of the virus. However, only low viral levels (below 10²) were present in most other organs and not detected in plasma at any time point ([Supplementary Figure 2](#)). This low viral RNA lacking replication in tissues could be detected by the presence of virus inoculated via multiple routes. Our qRT-PCR, with a primer and probe set specific for ORF1b, could not differentiate the reproducible viral RNA from inoculated viral RNA. Without exception, all macaques had a significant decrease in total lymphocytes counts, including CD4⁺ and CD8⁺ T cells, B cells, and NK cells at 1 dpi ([Figure 2A and 2B](#)). This loss was observed across naive and memory subpopulations of T and B cells ([Supplementary Figure 3](#)). However, our NHP model showed that these decreased values gradually recovered and returned to baseline at 7 dpi ([Figure 2A and 2B](#)). RNAseq analyses revealed that genes relevant to the viral response (such as those associated with cytokine/chemokine signaling) were

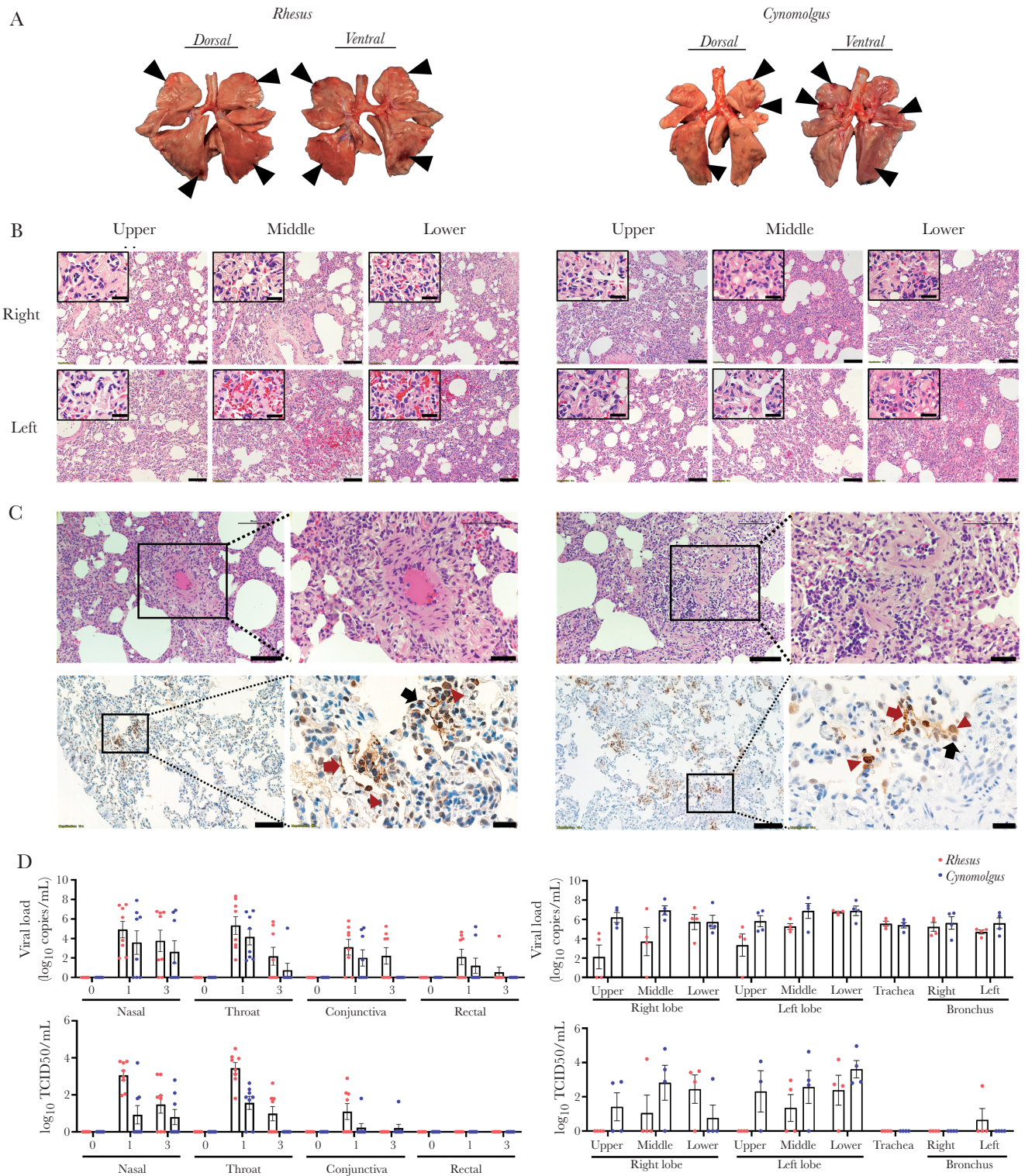
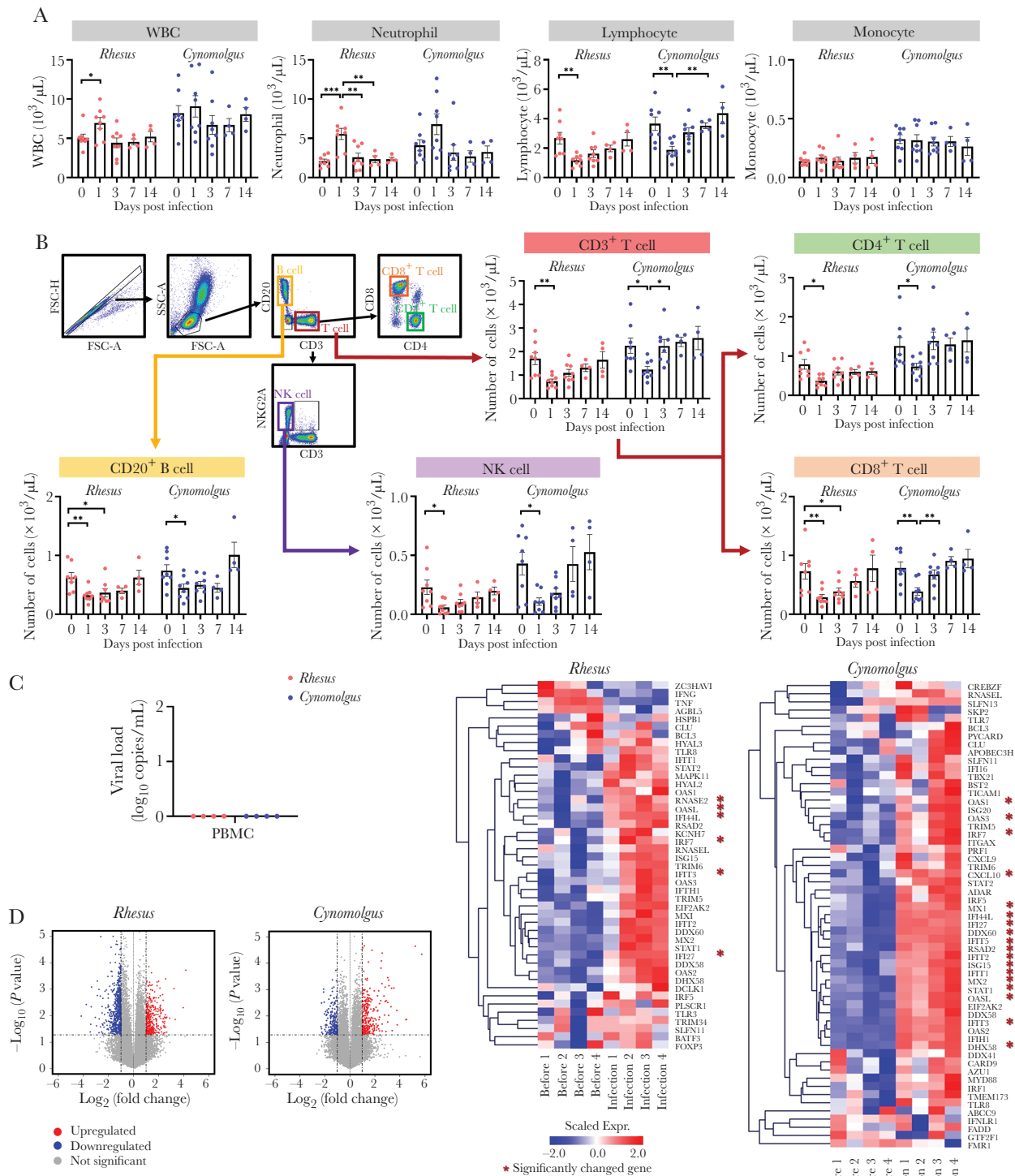


Figure 1. Pathological changes in macaques infected with SARS-CoV-2. Four rhesus and 4 cynomolgus macaques were euthanized at 3 dpi. *A*, Focal areas (black arrow head) of pulmonary consolidation in the lung lobes of macaques at 3 dpi. *B*, Histological analysis was performed on lobes (upper/middle/lower) of right and left lung in macaques. Scale bar, 100 μ m; inset, 20 μ m. *C*, There was apparent endothelial cell necrosis, as well as PMN and mononuclear leukocyte infiltration, in the intima of small and medium arterial vessels (H&E staining). Edema of the blood vessel walls and PMN and mononuclear cell infiltration around the blood vessels can be seen. Scale bar, 100 and 50 μ m in the left and right panels of each macaque species, respectively. Immunohistochemistry showed detection of SARS-CoV-2 antigen in the lungs. Scale bar, 100 μ m and 20 μ m. Type I pneumocytes (red arrow), type II pneumocytes (black arrow), and alveolar macrophage (red arrowhead). *D*, Swab samples and tissues were collected at 3 dpi and quantified for viral RNA (copies/mL) using qRT-PCR and TCID₅₀/mL. Mean \pm SEM. Abbreviations: SARS-CoV-2, severe acute respiratory syndrome coronavirus-2; dpi, days post infection; PMN, polymorphonuclear; qRT-PCR, quantitative reverse transcription polymerase chain reaction; TCID₅₀, median tissue culture infectious dose.



significantly elevated in PBMCs at 3 dpi, but no viral copies were detected (Figure 2C and 2D, Supplementary Table 1 and 2).

DISCUSSION

Here, we exposed NHPs to a high viral titer via combined routes, including the ocular route, nasal cavity, trachea, oral route, and blood, which have been reported as the possible routes of transmission [11–13], regardless of whether or not they are physiological routes. Using a high viral titer administered through combined routes, virus assays, and histopathological changes suggests that both cynomolgus and rhesus macaques are permissive to infection by SARS-CoV-2 and recapitulate COVID-19–like disease as in human. During early infection, acute interstitial pneumonia with endotheliitis was observed in the lungs of all infected macaques. Upper and lower respiratory tracts were the predominant sites of virus replication. This NHP model may also be suitable for investigating interactions between SARS-CoV-2 and the immune system. All macaques had a significant loss of total lymphocytes, including CD4⁺ and CD8⁺ T cells, B cells, and NK cells, during early infection. Similarly, lymphopenia was reported in 83.2% of hospitalized SARS-CoV-2 patients [14]. The alteration of peripheral lymphocyte subsets seems to be correlated with severe clinical cases [15]. Therefore, this NHP model of early infection may be used to validate the effect of immune modulators (eg, IL-7) in combination with therapeutic approaches to improve lymphopenia.

Supplementary Data

Supplementary materials are available at *The Journal of Infectious Diseases* online. Consisting of data provided by the authors to benefit the reader, the posted materials are not copyedited and are the sole responsibility of the authors, so questions or comments should be addressed to the corresponding author.

Notes

Acknowledgments. The authors thank the staff of the Korea National Primate Research Centre for their excellent veterinary care, Sanjeev Gumber (the director of Yerkes Histology and Molecular Pathology Laboratory at Emory) for his input on histological analysis, and Francois Villinger (the director of New Iberia Research Center) for productive discussions.

Author contributions. B. K., H. O., J. P., and J. J. H. analyzed the data and wrote the manuscript. B. K., H. O., G. K., E. H., H. J., P. K., Y. L., and J. J. H. performed experiments and managed animals. C. R. provided scientific input. J. J. H. was responsible for the concept and design of the study.

Financial support. This work was supported by the Ministry of Science and ICT of Korea (Korea Research Institute of Bioscience and Biotechnology Research Initiative Programs, grant numbers KGM 4572013 to J. J. H. and KGM2112032 to C.M. R.).

Potential conflicts of interest. All authors: No reported conflicts of interests. All authors have submitted the ICMJE Form for Disclosure of Potential Conflicts of Interest. Conflicts that the editors consider relevant to the content of the manuscript have been disclosed.

References

1. Wan Y, Shang J, Graham R, Baric RS, Li F. Receptor recognition by the novel coronavirus from Wuhan: an analysis based on decade-long structural studies of SARS coronavirus. *J Virol* **2020**; 94:e00127-20.
2. Fouchier RA, Kuiken T, Schutten M, et al. Aetiology: Koch's postulates fulfilled for SARS virus. *Nature* **2003**; 423:240.
3. Kuiken T, Fouchier RA, Schutten M, et al. Newly discovered coronavirus as the primary cause of severe acute respiratory syndrome. *Lancet* **2003**; 362:263–70.
4. Lawler JV, Endy TP, Hensley LE, et al. Cynomolgus macaque as an animal model for severe acute respiratory syndrome. *PLoS Med* **2006**; 3:e149.
5. Rowe T, Gao G, Hogan RJ, et al. Macaque model for severe acute respiratory syndrome. *J Virol* **2004**; 78:11401–4.
6. Rockx B, Kuiken T, Herfst S, et al. Comparative pathogenesis of COVID-19, MERS, and SARS in a nonhuman primate model. *Science* **2020**; 368:1012–5.
7. Munster VJ, Feldmann F, Williamson BN, et al. Respiratory disease in rhesus macaques inoculated with SARS-CoV-2 [published online ahead of print 12 May 2020]. *Nature* doi:10.1038/s41586-020-2324-7.
8. Chu DKW, Pan Y, Cheng SMS, et al. Molecular diagnosis of a novel coronavirus (2019-nCoV) causing an outbreak of pneumonia. *Clin Chem* **2020**; 66:549–55.
9. Tian S, Xiong Y, Liu H, et al. Pathological study of the 2019 novel coronavirus disease (COVID-19) through post-mortem core biopsies. *Mod Pathol* **2020**; 33:1007–14.
10. Varga Z, Flammer AJ, Steiger P, et al. Endothelial cell infection and endotheliitis in COVID-19. *Lancet* **2020**; 395:1417–8.
11. Wang W, Xu Y, Gao R, et al. Detection of SARS-CoV-2 in different types of clinical specimens. *JAMA* **2020**; 323:1843–4.
12. Xia J, Tong J, Liu M, Shen Y, Guo D. Evaluation of coronavirus in tears and conjunctival secretions of patients with SARS-CoV-2 infection. *J Med Virol* **2020**; 92:589–94.
13. Xiao F, Tang M, Zheng X, Liu Y, Li X, Shan H. Evidence for gastrointestinal infection of SARS-CoV-2. *Gastroenterology* **2020**; 158:1831–3.e3.
14. Guan WJ, Ni ZY, Hu Y, et al. Clinical characteristics of coronavirus disease 2019 in China. *N Engl J Med* **2020**; 382:1708–20.
15. Wang F, Nie J, Wang H, et al. Characteristics of peripheral lymphocyte subset alteration in COVID-19 pneumonia. *J Infect Dis* **2020**; 221:1762–9.